Materials International
Open Access Journal (ISSN: 2668-5728)

Article
Volume 6, Issue 4, 2024, 35
https://doi.org/10.33263/Materials64.035

Effect of Acetylene Monomers Conjugations upon Electronic, Linear/Nonlinear Optical Properties of Phosphorene Nanoflakes

Mohamed ElMansy [1,*]

[1] Condensed Matter Theory Group, Department of Physics, College of Science, Qassim University, Buraydah 51452, Saudi Arabia
* Correspondence: M.ElMansy@qu.edu.sa (M.E.)

Scopus Author ID: 35751222700
Received: 12.03.2024; Accepted: 7.07.2024; Published: 10.12.2024

Abstract: A virgin trial to boost electronic, linear/nonlinear characteristics of phosphorene-nanoflakes through conjugation with prototype conducting polymer such as polyacetylene has been fulfilled via DFT/B3LYP model. The phosphorene-acetylene (PA) conjugations are speculated via 3 probable conformations (armchair, end-edge, zigzag). The PA-zigzag exhibits a higher reactivity than both armchair and end-edged. PA-armchair & end-edged are preferred for fire-retardant sensories, while PA-zigzag is emerging as potential candidates for solar cells & avalanche photodetectors.

Keywords: density functional theory; electronic structure; optical properties; energy gap; polarization.

1. Introduction

In the last 10th years, phosphorene (P) $2D$-crystals have been recognized as advanced crystallographic models [1, 2] that possess an upgraded plane-in anisotropic character [3]. The surface nature of phosphorene is strongly folded and maintains a huge surface-to-volume ratio characteristic considering sp^3-crossover [4], which indicates high interaction of phosphorene with nearby molecules [5]. The P-nanoflakes are maintained in a planar configuration to enhance carriers' mobility and chemical reactivity [6]. The electronic characteristics and attributes of the P-nanoflakes can be conveniently altered by specific doping configurations[7]. In the context of gas sensing, the polarity and density of carriers in the P-nanoflakes have been evaluated by adsorbing gases such as O_2, NO_2, H_2O, CO_2 and NH_3 onto its surface[8]. Various papers have shed lights on applicability of P-nanostructures as an efficient channel for futured electronic technologies. The P-based FETs featuring $(Ti \sim 20\, nm\, \& SiO_2)$ established $electron/hole$ mobilities $\approx 38\, cm^2/Vs$ [10]. Also, nano-green-P doped by S reveals a remarkable shift in $I-V$ plot via NO_2 defiance, showing a prime applicability for chemogas sensing[11]. Manipulation across P-mechanical characteristics may be achieved via superficies sorption of Pt, Pd, Al, Li, Mg flags [12]. In addition, the manufactured Black P-based devices like gas sensing and supercapacitors are widely achnolwedged[13]. Moreover, Cycle for water spliting became more efficient upon Blue P-nanoribbons led [14]. A significant interest has been garnered for conducting polymers as a fresh electronic materials that sparked modern ideas for innovative technologies. Such conducting ploymers possess anisotropic quasi-1D configurations, setting them apart from conventional inorganic-based semiconductors. The

prime example of these conducting polymers is polyacetylene, PA. The idea of the present study is based upon conjugation between acetylene monomers and P-nanoflakes through 3 probable configurations (armchair, end-egde, zigzag). The implented acetylenes are forseesed to boost carriers mobility across P-nanoflakes, towards highly efficient photovoltaics era.

2. Materials and Methods

Theoretical iterations are accomplished by DFT/B3LYP interface considering the exact 6-31G(d,p) set enabled via Gaussian (G09) and GaussView 5.1 softcodes. The conjunctions between P-nanoflakes and acetylene monomers are set in 3 probable forms (armchair, end-edge & zigzag), constructing new PA nanoconjunctions. Imposed PA conjunctions are well optimized at the same level to check their stabilities, as appeared in Figure 1. Based upon Frontiers'energies (E_{HOMO}&E_{LUMO}), abundant parameters are computed like $E_{HOMO/LUMO}$ counterbalanced, ionizing-potential (IP), electronic-affinity (EA), chemical-potential (χ), hardness (κ), electrophile-index (ϕ), delicateness (s), and resultant dipole-moment (TDM) (see Table 1). Moreover, NLO indices like static-polarizability (α) and 1st hyper-polarizability (β) are calculated and embedded in Table 1.

3. Results and Discussion

3.1. Frontier molecular-orbitals (FMOs) analysis.

Many physical indices are derived from Frontiers' energies [38-41], as checked in Table 1. The checked indices identify the electronic change via acetylene conjunction upon P-nanoflakes. Only the zigzag conjunction is associated with TDM (2.64 D), whereas the armchair and end-edged conjunctions have TDMs that equal zero. The later P-conjunctions may be recognized as forthcoming fire-retardant sensories [42]. Based Si & Ge photovoltaics recently have carrier-duplication offsets 3.9 & 2.8 eV, respectively [43]. The $E_{HOMO/LUMO}$ offsets for P-conjunctions ranged from 3.34 ~ 3.39 eV, indicating potential photovoltaic nominee, especially for P-zigzags. The $E_{HOMO/LUMO}$ offsets for P-zigzags are 3.34 eV (see Figure 2). Domestically, P-zigzags may be competing rivals for upcoming solar cells [44, 45] and avalanche photodetectors[46-49].

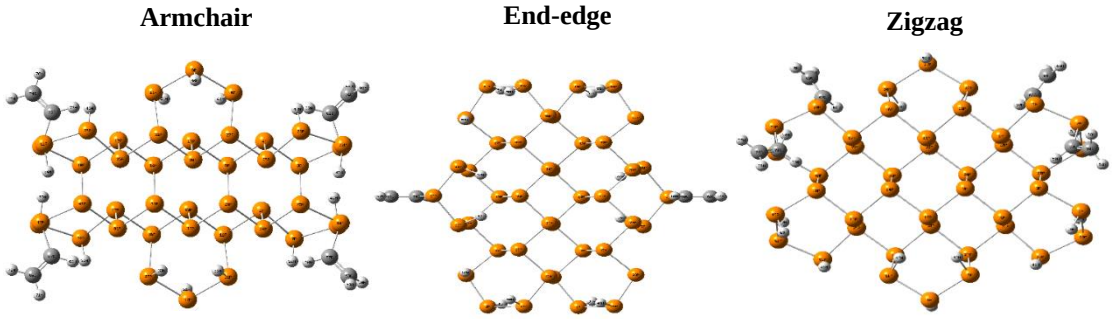

Figure 1. Optimum P-conjunctions via acetylene monomers.

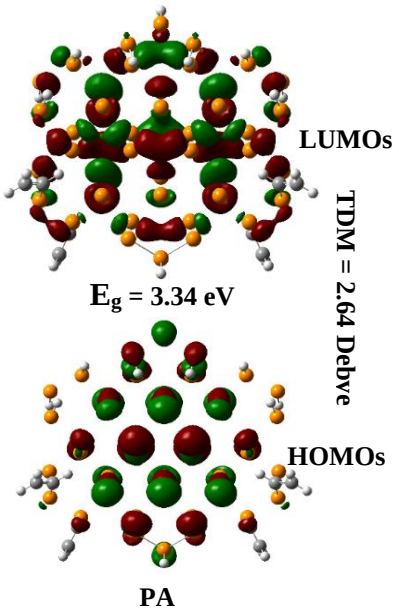

Figure 2. $E_{HOMO/LUMO}$ offsets for PA zigzag.

Table 1. E_{HOMO}, E_{LUMO}, $E_{HOMO/LUMO}$, ionizing potential, electronic affinity, chemical potential, hardenability, electrophile index, plasticity, and overall dipole moment for extrinsic P-nanoflakes.

	PA conjunctions		
	Armchair	***End-edge***	***Zigzag***
E_{LUMO} ***(eV)***	-2.48	-2.57	-2.53
E_{LUMO} ***(eV)***	-5.87	-5.89	-5.87
$E_{HOMO/LUMO}$ ***offset (eV)***	3.39	3.32	3.34
$IP = -E_{HOMO}$ ***(eV)***	5.87	0.22	0.22
$EA = -E_{LUMO}$ ***(eV)***	2.48	0.09	0.09
$\chi = \frac{E_{LUMO}+E_{HOMO}}{2}$ ***(eV)***	1.69	1.66	1.67
$\kappa = \frac{E_{LUMO}-E_{HOMO}}{2}$ ***(eV)***	-4.18	-4.23	-4.20
$\phi = \chi^2/2\kappa$ ***(eV)***	5.15	5.40	5.29
$S = 1/\kappa$ ***(eV^{-1})***	0.59	0.60	0.60
TDM (Debye)	0.00	0.00	2.64

3.1. NLO responses.

Focusing on P-zigzags, based on selected calculation level, NLO indices including static-polarizability (α_{tot}), anisotropic-polarizability ($\Delta\alpha$), and 1st hyperpolarizability (β_{tot}) are computed via mathematical forms [50-54]:

$$\alpha_{tot} = \frac{\alpha_{xx} + \alpha_{yy} + \alpha_{zz}}{3}$$

$$\Delta\alpha = \sqrt{\frac{(\alpha_{xx} - \alpha_{yy})^2 + (\alpha_{yy} - \alpha_{zz})^2 + (\alpha_{zz} - \alpha_{xx})^2 + 6\alpha_{yz}^2 + 6\alpha_{xy}^2 + 6\alpha_{xz}^2}{2}}$$

$$\beta_{tot} = \sqrt{(\beta_{xxx} + \beta_{xyy} + \beta_{xzz})^2 + (\beta_{yyy} + \beta_{yzz} + \beta_{yxx})^2 + (\beta_{zzz} + \beta_{zxx} + \beta_{zyy})^2}$$

where (α_{ij}) and (β_{ijk}) are polarizability and hyperpolarizability tensors, respectively. All calculated tensors are collected in Appendix A.

Table 2. Static-polarizability (α_{tot}), anisotropic-polarizability ($\Delta\alpha$), and 1st hyperpolarizability (β_{tot}) for P-zigzag via acetylene conjunctions.

	α_{tot} ($*10^{-24}$ esu)	$\Delta\alpha$ ($*10^{-24}$ esu)	β_{tot} ($*10^{-30}$ esu)	$\beta_{tot\,f} > \beta_{urea}$ [$\beta_{urea} = 0.3728 * 10^{-30}$ esu]
PA Zigzag	193.16	134.62	6.06	~16

Table 2 shows 1st hyperpolarizability (βtot), $\Delta\alpha$ *and* α_{tot} for P-zigzag. All obtained data are switched into esu scale (α; 1 a.u = 0.1482∗10−24 esu, β; 1 a.u = 8.6393∗10−33 esu). The P-zigzag via acetylene conjunctions has the highest βtot surpass16 times reference urea; βurea = 0.3728 x 10-30 esu. Such NLO response may be justified due to electron rush reducibility, which reproduces excitonic states inside the conduction domain. Eventually, we may announce P- zigzag via acetylene conjunctions as precious candidates for the future NLO era.

4. Conclusions

For the 1st time, electronic, linear/nonlinear optical responses of PA-nanoflakes are estimated theoretically via the DFT/B3LYP interface. The PA conjugations are designed via 3 probable configurations (armchair, end-edge, zigzag). Up to electronic and NLO response, P-zigzag surpasses armchair and end-edge ones. Both P-Armchairs and end-edges may be approved as the next fire-retardant sensories, while P-zigzag may compete for the next level of efficient solar cells and avalanche photodetectors.

Funding

This research received no external funding

Acknowledgments

Not applicable

Conflicts of Interest

The authors declare no conflict of interest

References

1. Kreno, L.E.; Leong, K.; Farha, O.K.; Allendorf, M.; Van Duyne, R.P.; Hupp, J.T. Metal–organic framework materials as chemical sensors. *Chemical reviews* **2012**, *112*, 1105-1125. https://doi.org/10.1021/cr200324t.
2. Goto, Y.; Sato, H.; Shinkai, S.; Sada, K. "Clickable" metal− organic framework. *Journal of the American Chemical Society* **2008**, *130*, 14354-14355. https://doi.org/10.1021/ja7114053
3. Zhu, Q.-L.; Xu, Q. Metal–organic framework composites. *Chemical Society Reviews* **2014**, *43*, 5468-5512. https://doi.org/10.1039/C3CS60472A.
4. Thorarinsdottir, A.E.; Harris, T.D. Metal–Organic Framework Magnets. *Chemical reviews* **2020**, *120*, 8716-8789. https://doi.org/10.1021/acs.chemrev.9b00666.
5. Lee, J.; Farha, O.K.; Roberts, J.; Scheidt, K.A.; Nguyen, S.T.; Hupp, J.T. Metal–organic framework materials as catalysts. *Chemical Society Reviews* **2009**, *38*, 1450-1459. https://doi.org/10.1039/B807080F.
6. Wei, Y.-S.; Zhang, M.; Zou, R.; Xu, Q. Metal–organic framework-based catalysts with single metal sites. *Chemical reviews* **2020**, *120*, 12089-12174. https://doi.org/10.1021/acs.chemrev.9b00757.
7. Wang, D.; Jana, D.; Zhao, Y. Metal–Organic Framework Derived Nanozymes in Biomedicine. *Accounts of Chemical Research* **2020**, *53*, 1389-1400. https://doi.org/10.1021/acs.accounts.0c00268.
8. Xu, G.-R.; An, Z.-H.; Xu, K.; Liu, Q.; Das, R.; Zhao, H.-L. Metal organic framework (MOF)-based micro/nanoscaled materials for heavy metal ions removal: The cutting-edge study on designs, synthesis, and

applications. *Coordination Chemistry Reviews* **2021**, *427*, 213554. https://doi.org/10.1016/j.ccr.2020.213554.
9. Xu, Y.; Wang, H.; Li, X.; Zeng, X.; Du, Z.; Cao, J.; Jiang, W. Metal–organic framework for the extraction and detection of pesticides from food commodities. *Comprehensive Reviews in Food Science Food Safety* **2021**, *20*, 1009-1035. https://doi.org/10.1111/1541-4337.12675.
10. Keller, N.; Bein, T. Optoelectronic processes in covalent organic frameworks. *Chemical Society Reviews* **2021**. https://doi.org/10.1039/D0CS00793E.
11. Li, C.; Zhang, C.; Xie, J.; Wang, K.; Li, J.; Zhang, Q. Ferrocene-based metal-organic framework as a promising cathode in lithium-ion battery. *Chemical Engineering Journal* **2021**, *404*, 126463. https://doi.org/10.1016/j.cej.2020.126463.
12. Wang, C.; Li, A.-R.; Ma, Y.-L. Phosphomolybdic acid niched in the metal-organic framework UiO-66 with defects: An efficient and stable catalyst for oxidative desulfurization. *Fuel Processing Technology* **2021**, *212*, 106629. https://doi.org/10.1016/j.fuproc.2020.106629.
13. Wang, X.; Chen, L.; Bai, Z.; Zhang, D.; Guan, J.; Zhang, Y.; Shi, C.; Diwu, J. In Vivo Uranium Sequestration using a Nanoscale Metal–Organic Framework. *Angewandte Chemie* **2021**, *133*, 1670-1674. https://doi.org/10.1002/ange.202012512.
14. Cao, S.-M.; Chen, H.-B.; Dong, B.-X.; Zheng, Q.-H.; Ding, Y.-X.; Liu, M.-J.; Qian, S.-L.; Teng, Y.-L.; Li, Z.-W.; Liu, W.-L. Nitrogen-rich metal-organic framework mediated Cu–N–C composite catalysts for the electrochemical reduction of CO2. *Journal of Energy Chemistry* **2021**, *54*, 555-563. https://doi.org/10.1016/j.jechem.2020.06.038.
15. Chen, L.; He, C.; Wang, R.; Li, Q.; Zeng, J.; Liu, W.; Wang, Y.; Wang, Q.; Ye, T.; Tang, Y. Potential active sites of Mo single atoms for electrocatalytic reduction of N2. *Chinese Chemical Letters* **2021**, *32*, 53-56. https://doi.org/10.1016/j.cclet.2020.11.013.
16. Farha, O.K.; Chen, Y.; Li, P. INSULIN-LOADED METAL-ORGANIC FRAMEWORKS. US Patent 11,666,637, Google Patents 2023. US11666637B2 - Insulin-loaded metal-organic frameworks - Google Patents
17. Chaudhary, K.P.; Patel, U.H.; Pandya, S.B.; Socha, B.N.; Padariya, T.J.; Alalawy, M.D.; Chavda, B.R.; Patel, R.; Patel, N.J.; Bhatt, B.S. Coordination behavior of succinylsulfathiazole–Crystal structure of [Cu (SST).(Pyridine) 3. H2O] n, DNA interaction and cytotoxic studies. *Journal of Molecular Structure* **2021**, *1225*, 129262. https://doi.org/10.1016/j.molstruc.2020.129262.
18. Bera, P.; Aher, A.; Brandao, P.; Manna, S.K.; Bhattacharyya, I.; Pramanik, C.; Mandal, B.; Das, S.; Bera, P. Synthesis, structure elucidation and dft study of a new thiazole–pyridine anchored nnn donor and it's cobalt (II) complex: In-vitro antitumor activity against U937 cancer cells, dna binding property and molecular docking study. *Journal of Molecular Structure* **2021**, *1224*, 129015. https://doi.org/10.1016/j.molstruc.2020.129015.
19. Li, D.; Zhan, P.; Liu, H.; Pannecouque, C.; Balzarini, J.; De Clercq, E.; Liu, X. Synthesis and biological evaluation of pyridazine derivatives as novel HIV-1 NNRTIs. *Bioorganic medicinal chemistry* **2013**, *21*, 2128-2134. https://doi.org/10.1016/j.bmc.2012.12.049
20. Mansour, E.; Abd-Rabou, A.A.; Nassar, I.F.; Elewa, S.I. Synthesis, Docking and Anticancer Evaluation of New Pyridine-3-Carbonitrile Derivatives. *Polycyclic Aromatic Compounds* **2021**, 1-22. https://doi.org/10.1080/10406638.2020.1870507.
21. Kozaki, R.; Kato, H. CANCER TREATMENT METHOD USING Trk INHIBITOR AND KINASE INHIBITOR IN COMBINATION. US Patent App. 16/643,988, Google Patents 2021. US20210000830A1 - CANCER TREATMENT METHOD USING Trk INHIBITOR AND KINASE INHIBITOR IN COMBINATION - Google Patents
22. Ma, R.; Tao, Y.; Chen, Y.; Liu, T.; Luo, Z.; Guo, Y.; Xiao, Y.; Fang, J.; Zhang, G.; Li, X. Achieving 16.68% efficiency ternary as-cast organic solar cells. *Science China Chemistry* **2021**, 1-9. https://doi.org/10.1007/s11426-020-9912-0
23. Long, X.; Tan, H.; Sánchez, F.; Fina, I.; Fontcuberta, J. Non-volatile optical switch of resistance in photoferroelectric tunnel junctions. *Nature communications* **2021**, *12*, 1-9. https://doi.org/10.1038/s41467-020-20660-9
24. Nirmala, A.; Mukkatt, I.; Shankar, S.; Ajayaghosh, A. Thermochromic Color Switching to Temperature Controlled Volatile Memory and Counter Operations with Metal–Organic Complexes and Hybrid Gels. *Angewandte Chemie International Edition* **2021**, *60*, 455-465. https://doi.org/10.1002/anie.202011580.
25. Wang, X.; Li, L.; Gu, X.; Yu, B.; Jiang, M. Switchable electrochemical aptasensor for amyloid-β oligomers detection based on triple helix switch coupling with AuNPs@ CuMOF labeled signaling displaced-probe. *Microchimica Acta* **2021**, *188*, 1-11. https://doi.org/10.1007/s00604-021-04704-5.
26. M. J. Frisch, G.W.T., H. B. Schlegel, G. E. Scuseria, M. A. Robb, J. R. Cheeseman, J. A. Montgomery, Jr., T. Vreven, K. N. Kudin, J.C. Burant, J. M. Millam, S.S. Iyengar, J. Tomasi, V. Barone, B. Mennucci, M. Cossi, G. Scalmani, N. Rega, G. A. Petersson, H. Nakatsuji, M. Hada, M.Ehara, K. Toyota, R. Fukuda, J. Hasegawa, M. Ishida, T. Nakajima, Y. Honda, O. Kitao, H. Nakai, M. Klene, X. Li, J. E. Knox, H.P.

Hratchian, J.B. Cross, C. Adamo, J. Jaramillo, R. Gomperts, R. E. Stratmann, O. Yazyev, A.J. Austin, R.Cammi, C. Pomelli, J.W. Ochterski, P.Y. Ayala, K. Morokuma, G.A. Voth, P. Salvador, J. J. Dannenberg, V.G. Zakrzewski, S. Dapprich, A.D. Daniels, M.C. Strain, O. Farkas, D.K. Malick, A.D. Rabuck, K. Raghavachari, J. B. Foresman, J. V. Ortiz, Q. Cui, A.G. Baboul, S. Clifford, J. Cioslowski, B. B. Stefanov, G. Liu, A. Liashenko, P. Piskorz, I. Komaromi, R.L. Martin, D.J.Fox, T. Keith, M. A. Al-Laham, C.Y. Peng, A. Nanayakkara, M. Challacombe, P. M. W. Gill, B. Johnson, W. Chen, M. W. Wong, C. Gonzalez, J. A. Pople. Gaussian09, Revision A. *Inc., Wallingford CT* 2009.

27. Frisch, A.; Dennington, R.; Keith, T.; Millam, J.; Nielsen, A.; Holder, A.; Hiscocks, J. Gauss view version 5 user manual. *Gaussian Inc., Wallingford, CT, USA* 2009, https://www.researchgate.net/publication/292069487_Gaussian_09_Revision_A1_Gaussian_Inc.
28. Tiama, T.M., Elhaes, H., Ibrahim, M.A. et al. Molecular and biological activities of metal oxide-modified bioactive glass. *Sci Rep* **2023**, *13*, 10637. https://doi.org/10.1038/s41598-023-37017-z29.
29. El-Mansy, M. Quantum chemical studies on structural, vibrational, nonlinear optical properties and chemical reactivity of indigo carmine dye. *Spectrochimica Acta Part A: Molecular Biomolecular Spectroscopy* **2017**, *183*, 284-290. https://doi.org/10.1016/j.saa.2017.04.047.
30. Soliman, H.; Ibrahim, M.; El-Mansy, M.; Atef, S.J.O.M. Structural and optical study of nanostructure of 4-cyanopyranoquinolinedione (CPQ) thin films. **2017**, *72*, 122-129. https://doi.org/10.1016/j.optmat.2017.05.052.
31. El-Mansy, M.; El-Bana, M.; Fouad, S. On the spectroscopic analyses of 3-Hydroxy-1-Phenyl-Pyridazin-6 (2H) one (HPHP): a comparative experimental and computational study. *Spectrochimica Acta Part A: Molecular Biomolecular Spectroscopy* **2017**, *176*, 99-105. https://doi.org/10.1016/j.saa.2016.12.040.
32. Gulácsi, M.; El-Mansy, M.; Gulácsi, Z.; Electron-phonon interactions in conducting polymers. *Philosophical Magazine Letters* **2016**, *96*, 67-75. https://doi.org/10.1080/09500839.2016.1150611.
33. Ibrahim, M.; El-Barbary, A.A.; El-Nahass, M.; Kamel, M.; El-Mansy, M.; Asiri, A.M.; On the spectroscopic analyses of (E)-3-(dicyclopropyl methylene)-dihydro-4-[1-(2, 5 dimethylfuran-3-yl) ethylidene] furan-2, 5-dione. *Spectrochimica Acta Part A: Molecular Biomolecular Spectroscopy* **2012**, *87*, 202-208. https://doi.org/10.1016/j.saa.2011.11.039.
34. El-Nahass, M.; Kamel, M.; El-Barbary, A.; El-Mansy, M.; Ibrahim, M.; FT-IR spectroscopic analyses of 3-Methyl-5-Pyrazolone (MP). *Spectrochimica Acta Part A: Molecular Biomolecular Spectroscopy* **2013**, *111*, 37-41. https://doi.org/10.1016/j.saa.2013.03.072.
35. El-Mansy, M.; El-Nahass, M.; Khusayfan, N.; El-Menyawy, E.M.; DFT approach for FT-IR spectra and HOMO–LUMO energy gap for N-(p-dimethylaminobenzylidene)-p-nitroaniline (DBN). *Spectrochimica Acta Part A: Molecular Biomolecular Spectroscopy* **2013**, *111*, 217-222. https://doi.org/10.1016/j.saa.2013.04.018.
36. El-Mansy, M.A.M.; Thanmayalaxmi, D.; Suvitha, A. et al. Crystallographic (X-rays), Spectroscopic (FT-IR, FT-Raman, NMR), electronic (NBO, FMOs) and NLO analyses for Zidovudine (ZDV); correlated experimental and theoretical studies. *Optical and Quantum Electronics* **2023**, *55*, 490. https://doi.org/10.1007/s11082-023-04728-6.
37. Khodair, A.I.; Kassab, S.E.; Kheder, N.A.; Fahim, A.M.; Synthesis of novel d-α-galactopyranosyl-l-seryl/l-threonyl-l-alanyl-l-alanine as useful precursors of new glycopeptide antibiotics with computational calculations studies. *Carbohydrated Research* **2022**, *514*, 108546. https://doi.org/10.1016/j.carres.2022.108546.
38. El-Mansy, M.A.M.; Bayoumy, A.M.; Elhaes, H. et al. Exploring the electronic, optical, and bioactive properties for new modified fullerenes via molecular modeling. *Optical and Quantum Electronics*, **2023**, *55*, 100 . https://doi.org/10.1007/s11082-022-04353-9.
39. Caramiello, A.M.; Bellucci, M.C.; Cristina, G.; Castellano, C.; Meneghetti, F.; Mori, M.; Secundo, F.; Viani, F.; Sacchetti, A.; Volonterio, A.; Synthesis and Conformational Analysis of Hydantoin-Based Universal Peptidomimetics. *Journal of Organic Chemistry* **2023**, *88*, 10381–10402. https://doi.org/10.1021/acs.joc.2c01903.
40. Shalaby, M.A.; Al-Matar, H.M.; Fahim, A.M.; Rizk, S.A.; A new approach to chromeno [4, 3-b] pyridine: Synthesis, X-ray, spectral investigations, hirshfeld surface analysis, and computational studies. *Journal of Physics and Chemistry of Solids* **2022**, *170*, 110933. https://doi.org/10.1016/j.jpcs.2022.110933.
41. Ibrahim, M.; El-Nahass, M.; Kamel, M.; El-Barbary, A.; Wagner, B.; El-Mansy, M.A.M.; On the spectroscopic analyses of thioindigo dye. *Spectrochimica Acta Part A: Molecular Biomolecular Spectroscopy* **2013**, *113*, 332-336. https://doi.org/10.1016/j.saa.2013.05.014.
42. Soliman, H.; Eid, K.M.; Ali, H.; El-Mansy, M.; Atef, S.; FT-IR spectroscopic analyses of 2-(2-furanylmethylene) propanedinitrile. *Spectrochimica Acta Part A: Molecular Biomolecular Spectroscopy* **2013**, *105*, 545-549. https://doi.org/10.1016/j.saa.2012.12.051.
43. Soliman, H.; Eid, K.M.; Ali, H.; Atef, S.; El-Mansy, M.A.M.; Vibrational spectroscopic analysis of 2-chloro-5-(2, 5-dimethoxy-benzylidene)-1, 3-diethyl-dihydro-pyrimidine-4, 6 (1H, 5H)-dione. *Spectrochimica Acta Part A: Molecular Biomolecular Spectroscopy* **2012**, *97*, 1079-1084. https://doi.org/10.1016/j.saa.2012.07.104.

44. Ismail, M.; Morsy, G.; Mohamed, H.; El-Mansy, M.A.M.; Abd-Alrazk, M.; FT-IR spectroscopic analyses of 4-hydroxy-1-methyl-3-[2-nitro-2-oxoacetyl-2 (1H) quinolinone (HMNOQ). *Spectrochimica Acta Part A: Molecular Biomolecular Spectroscopy* **2013**, *113*, 191-195. https://doi.org/10.1016/j.saa.2013.04.117.
45. El-Barbary, A.; El-Nahass, M.; Kamel, M.; El-Mansy, M.A.M. FT-IR, FT-Raman spectra and ab initio HF, DFT vibrational analysis of P-methyl acetanilide. *Journal of Applied Science Research* **2009**, *11*, 1977-1987, https://www.researchgate.net/publication/275658505_FT-IR_FT-Raman_Spectra_and_Ab_Initio_HF_DFT_Vibrational_Analysis_of_P-methyl_acetanilide.
46. Bayoumy, A.M.; Osman, Y.O.; Elhaes, H.; Ibrahim, M.A.; El-Mansy, M.A.M.; Effect of substitutions on the electronic properties of acetylsalicylic acid. *Optical Quantum Electronics* **2021**, *53*, 1-10. https://doi.org/10.1007/s11082-020-02725-7.
47. Zhang, Y.; Yuan, Y.; Cao, G.; Han, C.; Li, X.; Wang, X.; Zhang, G.; Geng, L.; Liu, W. A fresh-bias photoresponse of graphene field-effect transistor: An electrical tunable fast dipole moment generation. *Carbon* **2021**, *173*, 322-328. https://doi.org/10.1016/j.carbon.2020.11.022.
48. Sert, Y.; Sreenivasa, S.; Doğan, H.; Manojkumar, K.; Suchetan, P.; Ucun, F. FT-IR, Laser-Raman spectra and quantum chemical calculations of methyl 4-(trifluoromethyl)-1H-pyrrole-3-carboxylate-A DFT approach. *Spectrochimica Acta Part A: Molecular and Biomolecular Spectroscopy* **2014**, *127*, 122-130. https://doi.org/10.1016/j.saa.2014.02.069.
49. Das, T.; Rocquefelte, X.; Jobic, S. Ab Initio Positioning of the Valence and Conduction Bands of Bulk Photocatalysts: Proposition of Absolute Reference Energy. *The Journal of Physical Chemistry C* **2020**, *124*, 19426-19434. https://doi.org/10.1021/acs.jpcc.0c04003.
50. Cui, M.; Zheng, Z.; Wang, J.; Wang, Y.; Zhao, X.; Ma, R.; Liu, J. Rational design of Lithium-Sulfur battery cathodes based on differential Atom Electronegativity. *Energy Storage Materials* **2021**, *35*, 577-585. https://doi.org/10.1016/j.ensm.2020.11.039.
51. Kosar, N.; Ayub, K.; Mahmood, T. Surface functionalization of twisted graphene C32H15 and C104H52 derivatives with alkalis and superalkalis for NLO response; a DFT study. *Journal of Molecular Graphics Modelling* **2021**, *102*, 107794. https://doi.org/10.1016/j.jmgm.2020.107794.
52. Sathiya, S.; Senthilkumar, M.; Umarani, P. Synthesis, structural, spectroscopical and DFT studies on third order NLO crystal: Ethyl-5-hydroxy-4-(2-hydroxyphenyl)-2-oxo-6-(trifluoromethyl) hexahydropyrimidine5-carboxylate (EHOTHPC). *Journal of Molecular Structure* **2021**, *1224*, 129017. https://doi.org/10.1016/j.molstruc.2020.129017.
53. El-Mansy, M.; Osman, W.; Abdelsalam, H. The electronic and optical absorption properties of pristine, homo and hetero Bi-nanoclusters. *Chemical Physics Letters* **2021**, 111113. https://doi.org/10.1016/j.chemphys.2021.111113.
54. El-Mansy, M.; Ismail, M. Structural, conformational, optical, and nonlinear optical behavior of ethyl (6-ethyl 5, 6-dihydro 4, 5-dioxo 4 H pyrano [3, 2-c] quinolin-3yl) 2-oxoacetate (EPQOA): comparative theoretical and experimental studies. *Optical Quantum Electronics* **2021**, *53*, 1-19. https://doi.org/10.1007/s11082-021-02749-7.

Appendix A

Calculated polarizability α *(x10*$^{-24}$ *esu) and hyperpolarizability* β_{tot} *(x10*$^{-30}$ *esu) tensors for homo P-zigzags.*

	α_{xx}	α_{xy}	α_{yy}	α_{xz}	α_{yz}	α_{zz}	β_{xxx}	β_{xxy}	β_{xyy}	β_{yyy}	β_{xxz}	β_{xyz}	β_{yyz}	β_{xzz}	β_{yzz}	β_{zzz}
P-zigzag	259	0	214	0	4	107	0	2	0	4	-1	0	-1	0	0	0